Quantitative Analysis of Water Condensation in LP-EGR Systems for Internal Combustion Engines

Richárd Takács
Assistant lecturer
Széchenyi István University
Department of Vehicle Propulsion and Power Electronics
Audi Hungaria Faculty of Vehicle Engineering
Hungary

Jirí Vacula
Assistant Professor
Brno University of Technology
Institute of Automotive Engineering
Faculty of Mechanical Engineering
Czech Republic

Johan Prinsier
Senior Research Engineer
Von Karman Institute for Fluid Dynamics
Sint-Genesius-Rode
Belgium

Low-pressure exhaust gas recirculation (LP-EGR) is promising strategy for reducing NOx emissions in internal combustion engines, but it presents challenges due to water vapor condensation that can lead to compressor impeller erosion. This study presents a comprehensive thermodynamic analysis to quantify condensate formation and determine dew point temperatures across varying fuels and engine operating conditions. Novel mathematical models are developed to estimate specific humidity and condensation using only standard engine parameters, making them applicable without additional sensors. Results show that both fuel composition - particularly the hydrogen-to-carbon ratio - and LP-EGR rates strongly influence condensation. The study also highlights the impact of alternative fuels and ambient conditions on condensation risk. The developed methodology supports real-time evaluation of condensation potential and offers critical input for erosion risk assessment, component design, and emission control strategy optimization in modern powertrain.

Keywords: *Water vapor condensation, Alternative fuels, LP-EGR, Dew point temperature, Thermodynamic modelling.*

1. INTRODUCTION

According to the International Energy Agency's 2024 report, the transportation sector is responsible for 21% of global CO2 emissions, with road transport alone accounting for 11% [1]. These figures underscore the critical importance of developing environmentally focused strategies and technological solutions within the automotive industry. Contrary to earlier assumptions, it has now become evident that, in the short term, tailoring specific powertrain solutions to particular applications and use cases proves to be more effective than full electrification - especially when considering the total CO_2 emissions generated over a vehicle's entire life cycle, rather than only its local emissions [2–9]. In this context, it is clear that alongside the development of electric, fuel cell, and hybrid powertrains, the continued advancement of internal combustion engines remains of significant importance. However, in the case of internal combustion engine-based powertrains, the reduction of both NOx and CO_2 emissions remains a significant challenge to meet increasingly strict regional regulations [10,11]. The combined use of low-pressure exhaust gas recirculation (LP-EGR) and turbocharging offers an effective means of substantially reducing these emissions, which has led to their growing application in modern powertrains. Downsizing, enabled by turbocharging, leads to reduced engine displacement, which in turn lowers frictional losses and results in decreased specific fuel consumption [12,13]. LP-EGR technique, on the other hand, reduces peak combustion temperatures due to the presence of inert exhaust gases, thereby lowering NOx emissions [14,15]. Serrano et al. [16] identified several advantages and disadvantages of the LP-EGR system compared to the earlier applied HP-EGR techniques. Since there is no mass flow reduction on the turbine, there is no decrease in performance and a better transient response due to the faster buildup of boost pressure. Additionally, the system provides lower charge air temperatures and allows more time for the gases to mix before entering the cylinder, resulting in a significantly more homogeneous cylinder charge, as noted by Venu et al. [17] as well. Dimitriou et al. [18] identified an additional advantage of LP-EGR as it enables a higher mass flow through the turbocharger turbine, allowing the variable turbine geometry (VTG) to operate at a wider vane angle while maintaining the same boost pressure. This results in reduced exhaust backpressure and lower pumping losses, specifically in terms of piston displacement work. Furthermore, during cold ambient conditions, elevated NOx emissions can be observed shortly after engine start-up, prior to the catalytic converter reaching its optimal operating tem–perature. One of the key findings of Jung et al. [19] was that, in gasoline engines, exhaust gas recirculation (par–ticularly at part-load conditions) contributes to fuel con–sumption reduction. This is attributed to the increased throttle valve opening required to maintain the same power output when EGR rates are higher, thereby redu–cing throttling losses. This finding was confirmed by Bermúdez et al. [20] who demonstrated the same effect using testbench measurements methods. If the recir–culated exhaust gas is further cooled by an EGR cooler, the propensity for knock in spark-ignition (SI) engines can be substantially mitigated [21]. However, this concurrently increases the likelihood of water conden–

Received: July 2025, Accepted: November 2025
Correspondence to: Richárd Takács
Audi Hungária Faculty of Vehicle Engineering,
Egyetem tér 1, 9026 Győr, Hungary
E-mail: takacs.richard@ga.sze.hu
doi: 10.5937/fme2601001T

sation, potentially as early as the piping immediately downstream of the EGR cooler. However, the main disadvantages include a more expensive design due to the increased number of components, longer control response times resulting from extended piping, and the risk of mechanical damage to the compressor blades caused by accumulated water condensate. This latter phenomenon represents the most significant drawback, which has so far been the subject of only a few studies. Giechaskiel et at. [22] examines how water vapor con–densation during engine cold starts can distort exhaust gas measurements by diluting gas concentrations.

The research conducted by Siokos et al. [23] focused on quantifying the amount of water condensate formed under specific engine operating conditions, considering the quantity and temperature of the recirculated exhaust gas, as well as the ambient air temperature. The findings indicated that condensation is likely to occur when the exhaust gas is cooled below 53°C or when the ambient temperature drops below 0°C in conjunction with an EGR rate exceeding 8 %. However, the study does not investigate the influence of varying air-to-fuel ratios, LP-EGR pressure and its findings are limited to a single type of fuel. In addition, the effect of the pressure conditions within the LP-EGR duct on the condensation process remains unaddressed. Regarding the air-to-fuel ratio, Garrido et al. [24] also observed that using a stoichiometric mixture produces the highest amount of water condensate, as above this value a dilution effect occurs, whereas below it the amount of condensate decreases significantly due to the limited availability of fuel. However, they did not provide a corresponding mathematical description of this relationship. Serrano et al. [25] identified ambient air temperature, pressure, and humidity, as well as the LP-EGR aftercooler temperature, LP-EGR ratio, mixture pressure, and combustion process as key parameters influencing condensation formation. Their numerical results show good agreement with analytical calculations; however, beyond the presented figures and trends, no general mathematical formulation describing the condensation phenomenon was proposed.

It can be concluded that the application of LP-EGR offers significant potential for reducing NOx emissions and, in certain cases, improving fuel efficiency. However, the associated disadvantages—particularly the risk of water condensation—must be carefully considered. The high-velocity impingement of condensed water droplets on the compressor blades may lead to erosion or even catastrophic failure of the turbocharger's rotor system [26]. While several researchers have explored methods to reduce the extent of condensation, the complete elimination of this phenomenon under LP-EGR operation has not yet been achieved. An optimization strategy developed by Song et al. [27], based on a one-dimensional numerical model, demonstrated a 30.56% reduction in total condensation during a Worldwide harmonized Light vehicles Test Cycle (WLTC) without increasing NOx emissions. However, this came at the cost of a 1.13% rise in brake specific fuel consumption (BSFC), and no further details were provided regarding the impact on unburned hydrocarbon emissions. In parallel, Galindo et al. [28] investigated the mitigation of condensation through geometric optimization of the junction between the LP-EGR and the intake air duct. Their findings revealed that certain mixing ratios and junction angles can ensure that complete mixing of the gases occurs upstream of the compressor impeller's leading edge. It is important to note, however, that while such optimizations can effectively reduce condensation, the resulting flow patterns may adversely impact compressor efficiency, potentially leading to increased engine-specific fuel consumption [29].

The use of alternative fuels represents one of the most promising and actively researched areas in the field of internal combustion engine development. The primary objectives are to enhance the sustainability of fuel production and reduce CO_2 emissions, as demonstrated by numerous studies [30–32]. However, alongside the significant emissions benefits, several alternative fuels have been observed to increase the rate of water condensation, as previously discussed. Moroz et al. [33] demonstrated that, under stoichiometric conditions and equivalent energy release, the amount of condensed water is approximately 4% higher for soy and rapeseed oil and up to 8% higher for palm oil when compared to conventional diesel fuel. This increase is primarily attributed to the higher hydrogen-to-carbon ratio in the molecular structure of these bio-derived hydrocarbons. Similarly, d'Ambrosio et al. [34] investigated the combustion characteristics of hydrotreated vegetable oil (HVO) and found that its use enables higher LP-EGR rates compared to conventional diesel. This leads to an elevated water vapor content within the EGR loop, further increasing the likelihood of condensation.

The combustion of hydrogen also produces a significantly higher specific humidity than conventional hydrocarbon fuels. Since LP-EGR is similarly employed in hydrogen-fuelled internal combustion engines to reduce NOx emissions, the resulting high water vapor concentration can lead to an even greater risk of condensation and, consequently, droplet erosion of the turbocharger compressor impeller [35,36]. In summary, while the integration of alternative fuels with LP-EGR systems offers considerable benefits in terms of CO2 and NOx reduction, it also results in increased water condensation levels - posing a substantial challenge to component durability, particularly for the turbocharger compressor.

Although the phenomenon of condensation - emerging as one of the major drawbacks of LP-EGR systems - has been addressed in a few studies, the influence of several critical engine parameters remains insufficiently characterized, and the mathematical description of their impact on condensation is still incomplete. Identifying this research gap, the key objective of this article is to systematically investigate the engine-related factors influencing water condensation within LP-EGR systems and to develop mathematical models that quantitatively describe these relationships for any hydrocarbon-based fuel. During the formulation of the relationships, particular emphasis was placed on ensuring that the variables involved are parameters and/or input data that can be easily measured

in any internal combustion engine, to make the calculations applicable across different engine designs without the need for additional sensors.

2. METHODOLOGY

While the introduction refers to the occurrence of condensation, its specific locations - downstream of the LP-EGR cooler and upstream of the compressor impeller - are illustrated in the schematic layout in Figure 1 (locations 1 and 2, respectively).

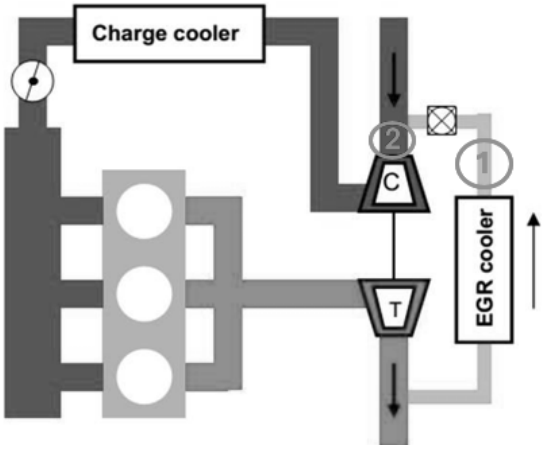

Figure 1. Potential water condensation locations within the LP-EGR system

The source of the condensation at Point 1 is the formation of water vapor during the combustion of hydrocarbons or hydrogen, which passes through the LP-EGR cooler where its temperature is significantly reduced. Under certain conditions, the medium can reach the saturation vapor pressure limit, resulting in condensation into liquid form. At Point 2, the relative humidity of the mixed ambient air and EGR gas can, in some cases, reach 100%, which also leads to condensation. This condensate may collide at high velocity with the compressor impeller, causing potential erosion. By knowing the specific humidity of the medium and the local dew point temperature, the presence and extent of condensation can be calculated. In internal combustion engines, the specific humidity of the exhaust gas (which is equal to the specific humidity of the LP-EGR flow) can be calculated based on the chemical equilibrium of the combustion process for the given operating condition. The second source of water formation is the specific humidity of the ambient air, which is governed by the ambient pressure and temperature, and can be determined as a function of these thermodynamic parameters. The specific humidity of these media deter–mines the amount of condensed water that may form. However, condensation occurs only at operating points where the media reach the dew point temperature at a gi–ven location, i.e., the condition of saturated vapor pressure.

2.1 Specific humidity calculation of the exhaust gas

To determine the specific humidity of the exhaust gas, it is necessary to calculate both the total mass of the exhaust gas and the mass of the water vapor generated during combustion. These quantities can be derived using the chemical equations describing the combustion process. It is important to note that, throughout this analysis, a complete combustion process and perfect mixing of air and fuel have been assumed. Of the components of air, only nitrogen, oxygen, and argon are considered in the calculations, as the mass fractions of the re–maining constituents are negligible. The coefficients for N_2 and Ar were determined based on their mass ratios relative to O_2 in dry air (dry air composition: 78.084 % N_2; 20.946 % O_2; 0.934 % Ar [37]).The method presented is valid exclusively for hydrocarbon and hydrogen fuels and assumes any air-to-fuel ratio. Under these conditions, the general combustion equation can be written as follows:

$$C_xH_y+\left(x+\frac{y}{4}\right)\left(O_2+3.73N_2+0.047Ar\right)= x\left(CO_2\right)+\frac{y}{2}\left(H_2O\right)+\left(x+\frac{y}{4}\right)\left(3.73N_2+0.047Ar\right) \quad (1)$$

The specific humidity of the exhaust (w_{exh}) gas in this case can be calculated as follows:

$$w_{exh_{\lambda=1}}=\frac{\frac{y}{2}\left(M_{H_2O}\right)}{x\left(MCO_2\right)+\frac{y}{2}\left(M_{H_2O}\right)+\left(x+\frac{y}{4}\right)\left(3.73M_{N_2}+0.047M_{Ar}\right)} \quad (2)$$

where M means the molecular weight of the different elements and molecules. During mixture enrichment (λ < 1), the combustion products also contain unburned hydrocarbons due to the limited availability of oxygen molecules, so the chemical combustion equation takes the following form:

$$C_xH_y+\lambda\left(x+\frac{y}{4}\right)\left(O_2+3.73N_2+0.047Ar\right)=\lambda x\left(CO_2\right)+\frac{\lambda}{2}\left(H_2O\right)+\lambda\left(x+\frac{y}{4}\right)\left(3.73N_2+0.047Ar\right)+\left(x-\lambda x\right)\left(C_xH_y\right) \quad (3)$$

The specific humidity of the exhaust gas in the case of a rich mixture can be calculated based on (4).

$$w_{exh_{\lambda<1}}=\frac{\lambda\frac{y}{2}\left(M_{H_2O}\right)}{\lambda x\left(MCO_2\right)+\lambda\frac{y}{2}\left(M_{H_2}O\right)+\lambda\left(x+\frac{y}{4}\right)\left(3.73M_{N_2}+0.047M_{Ar}\right)+\left(x-\lambda x\right)M_{C_xH_y}} \quad (4)$$

For a lean mixture (λ>1) combustion process, excess air is present (5). The specific humidity of the exhaust gas in the case of a lean mixture can be calculated based on (6). As can be seen from the above equations (1-6), the specific humidity of the exhaust gas is determined by the number of carbon and hydrogen atoms in the applied fuel, as well as by the air-to-fuel ratio used.

$$C_xH_y+\lambda\left(x+\frac{y}{4}\right)\left(O_2+3.73N_2+0.047Ar\right)=x\left(CO_2\right)+\frac{y}{2}\left(H_2O\right)+\lambda\left(x+\frac{y}{4}\right)\left(3.73N_2+0.047Ar\right)+\left(\left(x+\frac{y}{2}\right)\left(\lambda-1\right)\right)O_2 \quad (5)$$

$$w_{exh_{\lambda>1}} = \frac{\frac{y}{2}\left(M_{H_2O}\right)}{x\left(MCO_2\right)+\frac{y}{2}\left(M_{H_2}O\right)+\lambda\left(x+\frac{y}{4}\right)\left(3.73M_{N_2}+0.047M_{Ar}\right)+\left(\left(x+\frac{y}{2}\right)(\lambda-1)\right)M_{O_2}} \tag{6}$$

First, let us examine the effect of the hydrogen-to-carbon ratio in the case of a stoichiometric mixture (λ = 1). Figure 2 was created by substituting various carbon and hydrogen ratios, with several conventional fuels indicated as reference points.

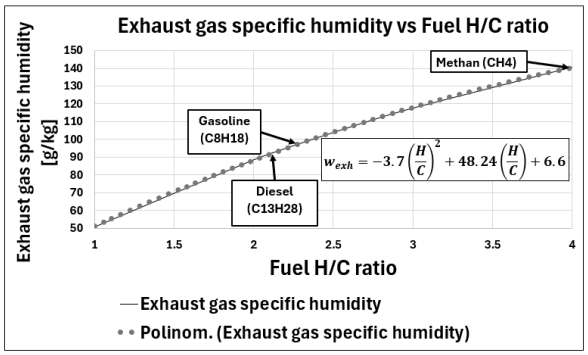

Figure 2. Exhaust gas specific humidity as a function of H/C ratio considering stochiometric mixture and perfect combustion

In this case, the lower limit of 1 on the x-axis corresponds to the theoretical minimum H/C ratio, which is characteristic of pure ethyne, while the upper limit of 4 represents the maximum achievable H/C ratio, corresponding to pure methane. In the case of hydrogen combustion, the H/C ratio is not applicable; however, the specific humidity of the exhaust gas at a stoichiometric air-fuel ratio can be calculated, and it is 339.22 g/kg. The specific humidity of the exhaust gas as a function of the H/C ratio can be approximated with high accuracy (R^2 = 0.9998) using the following second-degree polynomial function:

$$w_{exh} = -3.7\left(\frac{H}{C}\right)^2 + 48.24\left(\frac{H}{C}\right) + 6.6 \tag{7}$$

When applying the equation to conventional fuels under stoichiometric conditions, the highest specific humidity of the exhaust gas is observed for methane, which possesses the highest H/C ratio. Conversely, the lowest theoretical condensate formation occurs for diesel fuel, typically represented by the chemical composition $C_{13}H_{28}$, due to its lower H/C ratio.

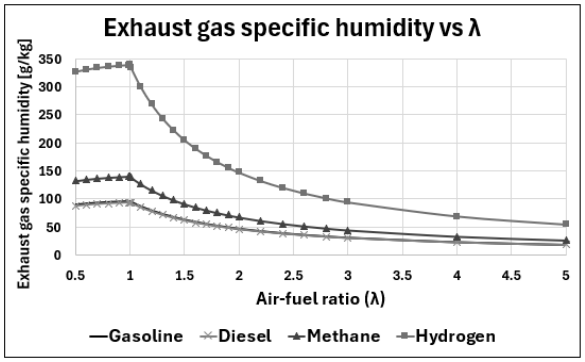

Figure 3. Exhaust gas specific humidity for various fuels as a function of the air–fuel equivalence ratio (λ).

The selection of the air-fuel ratio (λ) is a crucial parameter in determining the specific humidity of the exhaust gas during combustion, as it influences both the mass of water vapor generated and the total mass of the exhaust gas. By applying the previously described chemical equations under the assumption of complete combustion, the following relationship can be established for the specific humidity of the exhaust gas as a function of λ for representative fuels such as gasoline, diesel, methane, and hydrogen, as illustrated in Figure 3.

The highest specific humidity value occurs at the stoichiometric air-fuel ratio at any fuel. This can be explained by the fact that the mass of water vapor produced remains constant relative to the mass of fuel burned, while the total mass of the exhaust gas increases with mixture leaning, resulting in a gradual decrease in the water vapor proportion within the exhaust gas. Under rich mixture conditions, the exhaust gas contains unburned hydrocarbons that have not been converted to water vapor and CO_2, thereby reducing the relative proportion of water vapor compared to the burned fuel mass. It can be concluded that the specific humidity of the exhaust gas depends on the H/C ratio of the fuel used and the applied air-to-fuel ratio. For accurate determination, it is advisable to approximate the latter with at least a 5th-degree polynomial. In the case of using pure gasoline, for example, the following equation can be applied.

$$w_{exh\_gasoline} = 2.14x^5 - 30.13x^4 + 155.84x^3 - \\ -356.72x^2 + 318.78x + 1.5973 \tag{8}$$

Figure 4 illustrates the deviation of the fitted polynomial from the analytically calculated values at different fuels.

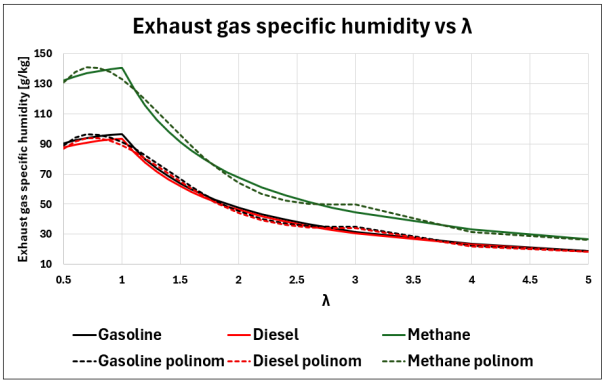

Figure 4. Exhaust gas specific humidity vs λ with fitted polynomials

As it can be seen in Figure 4, the 5th-order polynomial function fits the curve acceptably well over the entire λ range; however, this approach has several drawbacks. The most significant is that the maximum of the function does not occur at stoichiometric mixture (λ = 1), and it exhibits considerable deviations in the vicinity of this point. To address this issue, it is

advisable to divide the domain into two separate intervals: the first applied for $\lambda < 1$, and the second for $\lambda \geq 1$. The fitted polynomial functions obtained using this approach for gasoline are as follows:
The function applied in the case of $\lambda < 1$ ($R^2 = 0.9997$)

$$y = 2.77x^4 - 31.6x^3 + 136.68x^2 - 279.04x + 267.38 \quad (9)$$

The function applied in the case $\lambda < 1$ ($R^2 = 0.9993$)

$$y = -14.91x^2 + 34.46x + 76.94 \quad (10)$$

Figure 5 presents the extension of these functions forDiesel, Gasoline, and Methane.

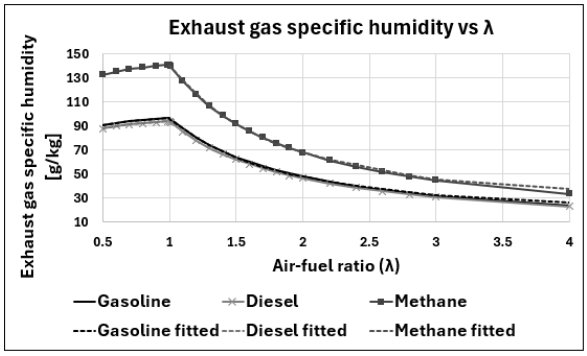

Figure 5. Polynomial fitting on exhaust gas specific humi–dity curves

As shown in Figure 5, the newly applied approach results in a much more accurate fit. Moreover, the previously observed issues - such as the location of the local maximum and the significant deviations around λ = 1 - have all been corrected.

The dependence of the exhaust gas specific humidity on both the H/C ratio and the lambda value has been established. By combining the effects of these variables, the specific humidity of the exhaust gas (a) in g/kg can be determined using a single general formula applicable for any hydrocarbon with a given hydrogen-to-carbon ratio (b) and air-to-fuel ratio (c) with high accuracy. For $\lambda < 1$ th e relationship can be defined in the following form:

$$a_1 = (-3.06b - 7.97)c^2 + (7.02b + 18.55)c + 21.35b + 28.69 \quad (11)$$

For $\lambda \geq 1$ the following formula can be used:

$$a_2 = (0.92b + 0.7)c^4 + (-1.0.36b - 8.21)c^3 + (43.98b + 37.38)c^2 + (-86.88b - 82.85)c + 77.51b + 92.25 \quad (12)$$

Using these functions, the complete characteristic field corresponding to the exhaust gas specific humidity can be constructed, as illustrated in Figure 6.

Figure 6 highlights several commonly used hydro–carbon fuels with dotted lines as references. It can be observed that, in all cases, the specific humidity of the exhaust gas reaches its maximum at λ = 1. Enriching the mixture causes this value to decrease gradually, whereas leaning the mixture results in a significantly steeper decline. The effect of the hydrogen-to-carbon (H/C) ratio of the fuel can also be observed.

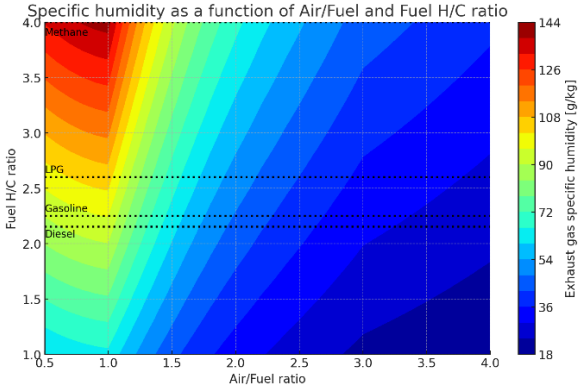

Figure 6. Characteristic map of exhaust gas specific humidity

The combustion of different fuels releases varying amounts of energy due to differences in their calorific values. Therefore, it is also important to assess the amo–unt of condensable water per unit of energy released. This enables a comparative evaluation of erosion risk associ–ated with different fuels, since higher condensate quan–tities correspond to increased erosion potential. Table 1 presents the exhaust gas specific humidity alongside the lower heating values (LHV) of various fuel mixtures at stoichiometric conditions and complete mixing. To esti–mate the amount of condensable water vapor per unit of released energy, the exhaust gas specific humidity is divi–ded by the calorific value of the respective fuel mixture.

Table 1. Comparison of the amount of condensable water vapor with the same energy released produced by different fuels combustion at λ = 1 in case of direct injection (DI)

Fuel	$w_{exh\lambda=1}$ [g/kg]	LHV_{mix} DI, λ = 1 [MJ/kg]	Cond. water [g/MJ]	Cond. water (gasoline eq.) [%]
Gasoline	96.52	2.83	34.11	100
Diesel	93.54	2.97	31.49	92.34
Methane	140.5	2.91	48.28	141.56
Hydrogen	339.22	3.51	96.64	283.36

Based on the data inTable 1, it can be observed that to release the same amount of energy (corresponding to the same load under real-driving conditions), diesel combustion produces 7.66% less condensate, methane combustion produces 41.56% more condensate, and hydrogen combustion produces 183.36% more con–densate compared to gasoline combustion.

2.2 Dew temperature calculation of the exhaust gas

The exhaust gas specific humidity for a given medium represents the maximum amount of water vapor that can potentially condense. However, condensation only occurs when the medium reaches saturation vapor pressure, which typically happens when the exhaust gas temperature falls below a certain threshold, namely the local dew point. One such scenario is during cold start and warm-up phases, where the engine and exhaust manifold operate at relatively low temperatures, causing the exhaust gas temperature to drop below the dew point. When an LP-EGR cooler is employed, this condition may arise already in the downstream pipe section.If the local dew point temperature of the exhaust

gas ($T_{dew\ exh}$) is to be determined, it is recommended to use the Magnus formula [38]:

$$T_{dew\_exh} = \frac{243.12 * \ln\left(\frac{e_{avp}}{6.112}\right)}{17.62 - \ln\left(\frac{e_{avp}}{6.112}\right)} \quad (13)$$

where e_{avp} is the actual vapour pressure, which can be calculated from the local pressure (here in the LP-EGR channel ($p_{lp\text{-}egr}$)) and the specific humidity of the ex–haust gas as follows:

$$e = \frac{p_{lp-egr} w_{exh}}{0.622 + w_{exh}} \quad (14)$$

Figure 7 represent an example (gasoline) how the exhaust gas pressure influences the dew temperature considering different lambda values.

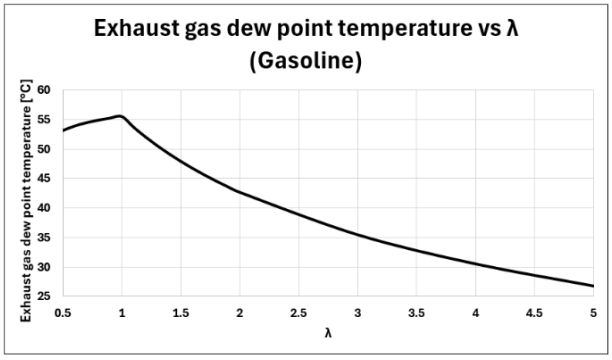

Figure 7. Exhaust gas dew point temperature vs λ (Gasoline)

By substituting the expression for the actual vapor pressure into the Magnus formula, and applying the specific humidity of the exhaust gas ($a_{1,2}$) in the previously defined form, the following complex equation is obtained:

$$T_{dew\_exh} = \frac{243.12 * \ln\left(\frac{p_{lp-egr} a_{1,2}}{6.112\left(0.622 + a_{1,2}/100\right)}\right)}{17.62 - \ln\left(\frac{p_{lp-egr} a_{1,2}}{6.112\left(0.622 + a_{1,2}/100\right)}\right)} \quad (15)$$

After applying the simplifications, the equation can be expressed in the following general form, where d is the dew point temperature of the exhaust gas, e is the exhaust gas pressure in the LP-EGR channel, and $a_{1,2}$ represent the previously defined specific humidity of the exhaust gas.

$$D = \frac{243.12 * \ln\left(\frac{e_{1,2}}{0.006 a_{1,2} + 3.8}\right)}{17.62 - \ln\left(\frac{e_{1,2}}{0.006 a_{1,2} + 3.8}\right)} \quad (16)$$

Based on equation 16, it can be concluded that the local dew point temperature of the exhaust gas can be determined from the local pressure value, the actual air-to-fuel ratio, and the composition of the fuel used.Using this equation, the highest exhaust gas dew point temperature for gasoline fuel is found to be 53.65°C at an exhaust gas pressure of 1.1bar and a stoichiometric air-fuel mixture. This result aligns closely with the findings of Hoppe et al. [39] and Garrido [24], who also reported a dew point temperature of approximately 53°C under stoichiometric conditions. However, their calculations considered only the N_2 and O_2 content of air and were limited to gasoline fuel.

Based on equation 15 and 16, the minimum tempe–rature can be determined above which the water content in the exhaust gas remains in the vapor phase, meaning that the relative humidity does not reach 100%. This parameter is critical when designing the cooling strategy for LP-EGR systems. Figure 8 presents a complete con–tour map illustrating the relationship of this value with the H/C ratio, λand exhaust gas pressure. For better visual representation, the pressure is displayed across six layers.

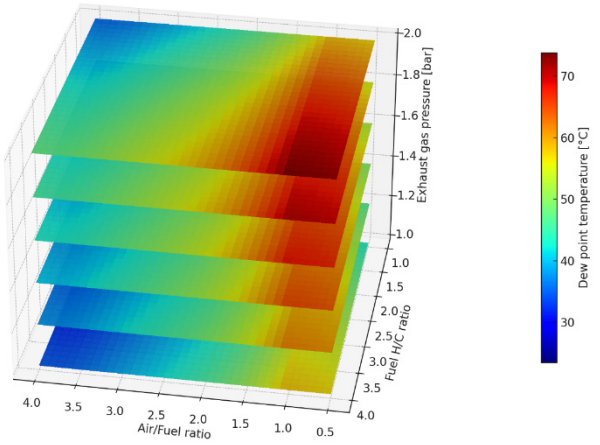

Figure 8. Exhaust gas dew point temperature contour map

As shown in Figure 8, the exhaust gas dew point temperature increases with higher H/C ratios in the fuel and higher exhaust gas pressure. Regarding lambda, the highest exhaust gas dew point temperature occurs at λ = 1. Leaning the mixture causes a significant decrease in dew point temperature, whereas enriching the mixture results in a more gradual decline of this parameter. Table 2 summarizes the dew point temperatures of dif–ferent fuels at an exhaust gas pressure of 1.1 bar.

Table 2. Comparison of exhaust gas dew point temperature for different fuels at stoichiometric mixture and 1.1 bar pressure in the LP-EGR channel.

	Gasoline	Diesel	Methane	Hydrogen
$T_{dew\text{-}egr}$	53.65°C	53.19°C	60.38°C	73.06°C

2.3 Specific humidity of the intake air and LP-EGR mixture

In LP-EGR systems, an additional potential source of condensation arises from the mixing of LP-EGR gas with intake air upstream of the turbocharger compressor. In this region, the blending of media with differing temperatures and specific humidity may result in a mixture whose temperature falls below the local dew point, leading to condensation of the water vapor present in the gas. Before analysing the thermodynamic

properties of the mixture, it is important to highlight that the ambient air drawn into the engine also contains condensable amount of water vapor, characterized by the specific humidity of the medium. The extent of this humidity is determined by the atmospheric temperature and pressure, which define the saturation pressure and the actual partial pressure of water vapor. Figure 9 illustrate the relationship between ambient temperature and ambient specific humidity at a constant atmospheric pressure and a fixed relative humidity of 20% covering the broadest range of conditions typically encountered in real-world transportation scenarios. Additionally, Figure 10 shows the relationship between ambient pressure and specific humidity at a constant temperature of 25 °C and a relative humidity of 20%. The purpose of the presentation of Figure 9 and 10 is to depict the general trends of how these environmental parameters influence specific and specific humidity under typical operating conditions.

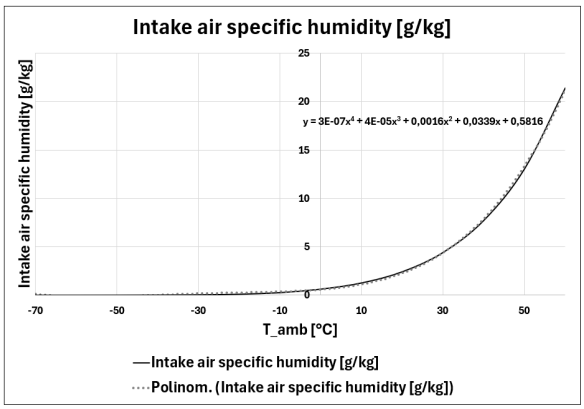

Figure 9.Intake air specific humidity as a function of ambient air temperature (atmospheric pressure)

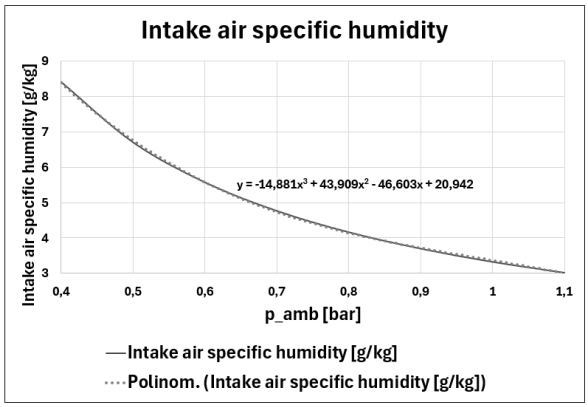

Figure 10. Intake air specific humidity as a function of ambient pressure (T_{amb} = 25°C)

It can be observed that changes in temperature have a significantly greater effect on the ambient air specific humidity than changes in pressure. If relative humidity is also considered, the relationships shown in Figure 11 (presented in the Appendix) can be used. It is evident that as temperature and relative humidity increase, the specific humidity rises markedly. In extreme cases (e.g., 40°C and 90% relative humidity), the ambient air specific humidity can reach values comparable to those of exhaust gas specific humidity, making it an important factor to consider.

To determine the specific humidity of the mixture resulting from the combination of LP-EGR gas and intake air, with differing temperatures and specific humidity the individual specific humidities and mass flow rates must be weighted and combined according to the following equation.

$$w_{mix} = \frac{\dot{m}_{amb} w_{amb} + \dot{m}_{LP-EGR} w_{exh}}{\dot{m}_{amb} + \dot{m}_{LP-EGR}} \tag{17}$$

In internal combustion engines, the measurement of intake air mass flow is a key factor for engine operation and is therefore always performed. In contrast, direct sensor-based measurement of the exhaust gas mass flow is uncommon due to the high thermal load and increased cost. Instead, the engine control unit typically determines it indirectly, using a ratio based on the EGR valve opening angle. In the case of LP-EGR systems, this ratio can be described by Equation 18.

$$LP-EGR\,ratio = \frac{\dot{m}_{LP-EGR}}{\dot{m}_{amb} + \dot{m}_{fuel}} \tag{18}$$

By substituting this into Equation 17, give the name of *R* LP-EGR ratio and using the previously defined $a_{1,2}$ to represent the exhaust gas specific humidity, the following combined equation is obtained:

$$w_{mix} = \frac{\dot{m}_{amb} w_{amb} + \left(R\left(\dot{m}_{mb} + \dot{m}_{fuel}\right)\right) a_{1,2}}{\dot{m}_{amb} + \left(R\left(\dot{m}_{amb} + \dot{m}_{fuel}\right)\right)} \tag{19}$$

In general form, the equation can be written as fol–lows:

$$f = \frac{gh + \left(R\left(g+i\right)\right) a_{1,2}}{g + \left(R\left(g+i\right)\right)} \tag{20}$$

It can be stated that the specific humidity of the mixture (*f*) depends on the ambient air mass flow (*g*), the specific humidity of the ambient air (*h*), the LP-EGR ratio (*r*), the injected fuel mass flow (*i*), and the specific humidity of the exhaust gas ($a_{1,2}$). Since the latter two have already been determined, it can be concluded that, by applying the presented mathematical models, the specific humidity of the medium present upstream of the compressor wheel can be calculated based on the following parameters: ambient air mass flow, ambient air temperature, ambient air pressure, ambient air relative humidity, LP-EGR ratio, injected fuel mass flow, H/C ratio of the fuel, and the air–fuel ratio. Each of these parameters can be easily determined and mea–sured using sensors commonly installed in modern engines. The calculations presented therefore offer the possibility to provide real-time information about the extent of condensation under any engine operating con–ditions using any hydrocarbon-based fuel. A further im–portant aspect of the above-described equation is the mixture specific humidity dependency from LP-EGR ratio. The example illustrated in Figure 12 demonstrates the variation of the mixture's specific humidity as a function of the LP-EGR ratio, assuming constant ambi–ent conditions and mass flow rate for gasoline fuel at stoichiometric combustion.

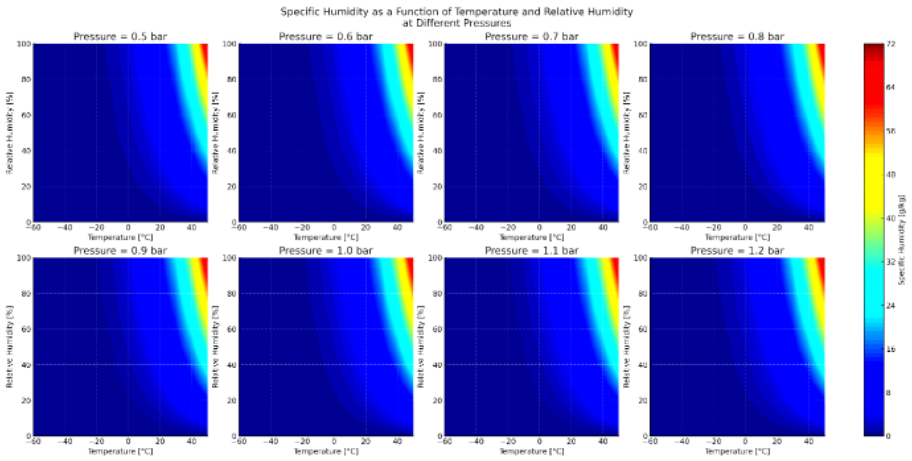

Figure 11. Ambient air specific humidity as a function of ambient temperature, relative humidity and ambient pressure

As shown in Figure 12, the specific humidity of the mixture increases significantly with the rise in the LP-EGR ratio. This is highly relevant in the context of current engine development trends, as the gradual reduction of NO_x emissions involves an increasing recirculation of exhaust gas [40,41]. However, this also leads to a higher potential for condensation, thereby increasing the risk of damage to the compressor impeller.

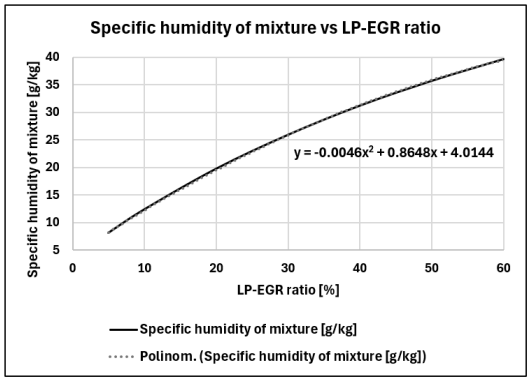

Figure 12. Specific humidity of the mixture vs LP-EGR ratio

2.4 Dew temperature calculation of the LP-EGR and intake air mixture

Condensation of the water vapor present in the medium will only occur if the temperature of the resulting mixture falls below the local dew point. The temperature of the mixture can be determined based on the mass flow rate, temperature, and specific heat capacity of the contributing media.

$$T_{mix} = \frac{\dot{m}_{amb} c_{amb} T_{amb} + \dot{m}_{LP-EGR} c_{exh} T_{exh}}{\dot{m}_{amb} c_{amb} + \dot{m}_{LP-EGR} c_{exh}} \tag{21}$$

The commonly used value for the specific heat capacity of air is 1010J/kgK, while the specific heat capacity of exhaust gas resulting from hydrocarbon combustion can be taken as 1100 J/kgK. The latter value depends on the air–fuel ratio and the prevailing temperature; however, within the narrow LP-EGR cooler outlet temperature range typically observed in practice (300–500°K), it does not exhibit significant variation [42]. By substituting these values, along with the LP-EGR ratio, the following equation is obtained:

$$T_{mix} = \frac{\dot{m}_{amb} * 1010 * T_{amb} + \left(R\left(\dot{m}_{amb} + \dot{m}_{fuel}\right)\right) * 1100 * T_{exh}}{\dot{m}_{amb} * 1010 + \left(R\left(\dot{m}_{amb} + \dot{m}_{fuel}\right)\right) * 1100} \tag{22}$$

The local dew point temperature in this mixing area ($T_{dew\ mix}$) can be calculated using the Magnuss-formula [38] introduced earlier, considering the local pressure (p_{mix}), which is typically the combined effect of the LP-EGR system pressure, and the vacuum generated by the turbocharger at the given operating condition:

$$T_{dew\_mix} = \frac{243.12 * \ln\left(\frac{e_{avp}}{6.112}\right)}{17.62 - \left(\frac{e_{avp}}{6.112}\right)} \tag{23}$$

where e_{avp} is the actual vapour pressure, which can be calculated from the local pressure (here in the mixing channel (p_{max})) and the specific humidity of the mixture as follows:

$$e = \frac{p_{mix} w_{mix}}{0.622 + w_{mix}} \tag{24}$$

By combining the previous two equations, expanding the expression for the specific humidity of the mixed medium (w_{mix}) and using $a_{1,2}$ to represent the exhaust gas specific humidity, the (25) complex equation is obtained:

$$T_{dew\_mix} = \frac{243.12 * \ln\left(\frac{p_{mix}\left(\dot{m}_{amb} w_{amb} + R\left(\dot{m}_{amb} + \dot{m}_{fuel}\right) a_{1,2}\right)}{6.112\left(\dot{m}_{amb} w_{amb} + R\left(\dot{m}_{amb} + \dot{m}_{fuel}\right) a_{1,2}\right) + 3.8\left(\dot{m}_{amb} w_{amb} + R\left(\dot{m}_{amb} + \dot{m}_{fuel}\right)\right)}\right)}{17.62 - \ln\left(\frac{p_{mix}\left(\dot{m}_{amb} w_{amb} + R\left(\dot{m}_{amb} + \dot{m}_{fuel}\right) a_{1,2}\right)}{6.112\left(\dot{m}_{amb} w_{amb} + R\left(\dot{m}_{amb} + \dot{m}_{fuel}\right) a_{1,2}\right) + 3.8\left(\dot{m}_{amb} w_{amb} + R\left(\dot{m}_{amb} + \dot{m}_{fuel}\right)\right)}\right)} \tag{25}$$

In general form, the equation can be written as follows:

$$j=\frac{243.12*\ln\left(\frac{k\left(gh+R(g+i)a_{1,2}\right)}{6.112\left(gh+R(g+i)a_{1,2}+3.8\left(g+R(g+i)\right)\right)}\right)}{17.62-\ln\left(\frac{k\left(gh+R(g+i)a_{1,2}\right)}{6.112\left(gh+R(g+i)a_{1,2}+3.8\left(g+R(g+i)\right)\right)}\right)} \quad (26)$$

The true significance of equations 25 and 26 lies in the fact that it includes only parameters that are easily measurable and typically available in all engines, either through sensors or as calculated variables. Therefore, the dew point temperature in the pre-compressor region can be continuously monitored in real time.

If condensation occurs - i.e., if the mixture temperature drops below the local dew point temperature - the amount of resulting condensate can be calculated using Equation 27. This represents a highly important piece of information, as it constitutes one of the key input parameters for future erosion studies.

$$\dot{m}_{cond}=\left(\dot{m}_{amb}+\dot{m}_{LP-EGR}\right)w_{mix} \quad (27)$$

By reapplying the formula for the LP-EGR ratio (R), the equation can be transformed into the following form to ensure that all its parameters can be directly measured in a conventional internal combustion engine.

$$\dot{m}_{cond}=\left(\dot{m}_{amb}+R\left(\dot{m}_{amb}+\dot{m}_{fuel}\right)\right)w_{mix} \quad (28)$$

3. DISCUSSION

The aim of the presented zero-dimensional (0-D) quantitative analysis is to quantify the amount of condensable water generated in LP-EGR systems and to define the local dew point temperature across all load conditions and for various hydrocarbon and hydrogen fuels. This provides essential information not only for erosion testing and the manufacturing of turbocharger compressor wheels but also for optimizing the control strategies of LP-EGR systems, which directly influence pollutant emission levels from the powertrain. Furthermore, the developed mathematical functions can be implemented in simulation software that models combustion processes in internal-combustion engines, exhaust-gas analysis, and the prediction of condensation phenomena. They can also be coupled with selective diagnostics, such as those developed by Shepelev et al. [43], to interpret condition-dependent changes in exhaust composition and to support corrective control strategies.

In addition to the results reported in this research, the presented method is suitable for a comprehensive investigation of various environmental and combustion parameters (such as temperature, pressure, air-fuel ratio, fuel content, LP-EGR pressure and LP-EGR ratio) and their influence on condensation phenomena within the exhaust channels of internal combustion engines. This method also allows quantification of the amount of condensable water vapor produced during the combustion of any hydrocarbon or hydrogen–air mixture by calculating the exhaust gas specific humidity. This method also permits comparison of the amount of condensable water vapor produced during the combustion of different fuels releasing the same amount of energy. It was observed that, for the same energy output (corresponding to the same torque under real-driving conditions), diesel combustion produces 7.66 % less condensate, methane combustion produces 41.56 % more, and hydrogen combustion produces 183.36 % more condensate compared to gasoline combustion.

4. CONCLUSION

The analysis revealed that fuels with a higher hydrogen-to-carbon ratio (b) generate greater specific humidity, while the air-fuel ratio (c) has also a significant effect on it. It reaches its maximum at stoichiometric mixture. As the mixture is gradually enriched, the specific humidity decreases slightly, whereas with mixture depletion, it decreases more significantly This behaviour is described by two equations: a_1 provides a highly accurate approximation for $\lambda < 1$, while a_2 yields a precise approximation for $\lambda \geq 1$.

$$a_1=\left(-3.06b-7.97\right)c^2+\left(7.02+18.55\right)c+21.35b+28.69$$

$$a_2=\left(0.92b+0.7c\right)^4+\left(-10.36b-8.21\right)c^3+\left(43.98b+37.38\right)c^2+\left(-86.88b-82.85\right)c+77.51b+92.25$$

This research has also yielded that the dew temperature of the exhaust gas (d) is influenced by the pressure in the LP-EGR channel (e) and the exhaust gas specific humidity ($a_{1,2}$) and can be calculated by using the following formula:

$$d=\frac{243.12*\ln\left(\frac{ea_{1,2}}{6.112\left(0.622+a_{1,2}/1000\right)}\right)}{17.62-\ln\left(\frac{ea_{1,2}}{6.112\left(0.622+a_{1,2}/1000\right)}\right)}$$

The specific humidity of the medium (f) formed by the mixing of LP-EGR and intake air can be determined using the following equation, based on the intake ambient air mass flow (g), the specific humidity of the ambient air (h), the LP-EGR ratio (R), the fuel mass flow (i), and the exhaust gas specific humidity ($a_{1,2}$).

$$f=\frac{gh+\left(R\left(g+i\right)\right)a_{1,2}}{g+\left(R\left(g+i\right)\right)}$$

The dew point temperature of the mixture (j) resulting from the combination of LP-EGR and intake air can be determined using the following equation, based on the pre-compressor pressure (k), intake ambient air mass flow (g), ambient air specific humidity (h), LP-EGR ratio (R), fuel mass flow (i), and exhaust gas specific humidity ($a_{1,2}$).

$$j=\frac{243.12*\ln\left(\frac{k\left(gh+R\left(g+i\right)a_{1,2}\right)}{6.112\left(gh+R\left(g+i\right)a_{1,2}\right)+3.8\left(g+R\left(g+i\right)\right)}\right)}{17.62-\ln\left(\frac{k\left(gh+R\left(g+i\right)a_{1,2}\right)}{6.112\left(gh+R\left(g+i\right)a_{1,2}\right)+3.8\left(g+R\left(g+i\right)\right)}\right)}$$

ACKNOWLEDGMENT

This article is published in the framework of the project "Production and Validation of Synthetic Fuels in Industry-University Collaboration", project number "ÉZFF/956/2022-ITM_SZERZ".

REFERENCES

[1] International Energy Agency. Global Energy Review 2025: CO_2 Emissions. available: https://www.iea.org/reports/global-energy-review-2025-co2 -emissions

[2] Peters, J.F., Burguillo, M., Arranz, J.M.: Low emi–ssion zones: Effects on alternative-fuel vehicle up–take and fleet CO_2 emissions. Transportation Rese–arch Part D: Transport and Environment, 95, 102882, 2021. https://doi.org/10.1016/j.trd.2021.102882.

[3] Pacura, W., Szramowiat-Sala, K., Gołaś, J.: Emis–sions from light-duty vehicles From statistics to emission regulations and vehicle testing in the European Union. Energies, 17, 1, 209, 2024. https://doi.org/10.3390/en17010209.

[4] Ravi, S.S., Osipov, S., Turner, J.W.G.: Impact of modern vehicular technologies and emission regu–lations on improving global air quality. Atmos–phere, 14, 7, 1164, 2023. https://doi.org/10.3390/atmos14071164.

[5] Zhong, H., Chen, K., Liu, C., Zhu, M., and Ke, R.: Models for predicting vehicle emissions: A comprehensive review. Science of the Total Environment, 923, 171324, 2024. https://doi.org/10.1016/j.scitotenv.2024.171324.

[6] Tipton, M.J., Lathem, T.L., Fu, J.S., Tschantz, M.F.: Effectiveness of emissions standards on auto–motive evaporative emissions in Europe under normal and extreme temperature conditions. Envi–ronmental Research Communications, 4, 8, 081003, 2022. https://doi.org/10.1088/2515-7620/ac8b69.

[7] Li, X., Nam, K.-M.: Environmental regulations as industrial policy: Vehicle emission standards and automotive industry performance. Environmental Science and Policy, 131, 68–83, 2022. https://doi.org/10.1016/j.envsci.2022.01.015.

[8] Zheng, X., Chai, Q., Chen, Y., Li, X.: Assessing the GHG mitigation effect of the National VI Emis–sions Standard for light duty vehicles in China. Environmental Science and Pollution Research, 30, 36–43, 2023. https://doi.org/10.1007/s11356-022-24114-1.

[9] Csutora, M., Vetőné Mózner, Zs.: Carbon manage–ment strategies of the automotive sector responding to the European fleet-wide CO_2 emission targets. Discover Sustainability, 6, 346, 2025. https://doi.org/10.1007/s43621-025-01109-9.

[10] Zhang, S., Nie, X., Bi, Y., Yan, J., Liu, S., Peng, Y.: Experimental study on NO_x reduction of diesel engine by EGR coupled with SCR. ACS Omega, 9, 7, 8308–8319, 2024. https://doi.org/10.1021/acsomega.3c09052.

[11] Sandhu, N., Yu, X., Zheng, M.: Catalytic NO*x* Aftertreatment—Towards Ultra-Low NO*x* Mobility. International Journal of Automotive Manufacturing and Materials, 3, 1, 4, 2024. https://doi.org/ 10.53941/ijamm.2024.100004.

[12] Namara, M.M., Jahanian, O., Shafaghata, R., and Nikzadfara, K.: Numerical/Experimental Studies on Performance at Low Engine Speeds: A Case Study of Downsized Iranian National Engine (EF7). International Journal of Engineering – Transactions C: Aspects, 34, 9, 2138–2147, 2021.

[13] Namar, M.M., et al.: The comparative performance study of the EF7 downsized engines: Fuel economy besides CO_2 reduction. Future Technology, 3, 3, 20–32, 2024. https://doi.org/10.55670/fpll.futech.3.3.4.

[14] Lapuerta, M., Ramos, Á., Fernández-Rodríguez, D., and González-García, I.: High-pressure versus low-pressure exhaust gas recirculation in a Euro 6 diesel engine with lean-NOx trap: Effectiveness to reduce NOx emissions. International Journal of Engine Research, 20, 1, 155-163, 2018. https://doi.org/ 10.1177/1468087418817447.

[15] Chen, X., Jiang, Y., Zhao, Z.: Prediction of com–bustion and exhaust emission of a CI engine fueled with diesel-biodiesel blends with different EGR rates. Frontiers in Energy Research, 11, 1205840, 2023. https://doi.org/10.3389/fenrg.2023.1205840.

[16] Serrano, J.R., Piqueras, P., Navarro, R., Tarí, D., Meano, C.M.: Development and verification of an in-flow water condensation model for 3D-CFD simulations of humid air streams mixing. Compu–ters and fluids 167, 158-165, 2018.

[17] Venu, H., Subramani, L., Raju, D.V.: Emission reduction in a DI diesel engine using exhaust gas recirculation (EGR) of palm biodiesel blended with TiO2 nano additives. Renewable Energy, 140, 245-263, 2019. https://doi.org/10.1016/j.renene.2019.03. 078.

[18] Dimitriou, P., Turner, J., Burke, R., Copeland, C.: The benefit of a mid-route exhaust gas recirculation system for two-stage boosted engines. International Journal of Engine Research, 19, 5, 553-569, 2017. https://doi.org/10.1177/1468087417723782.

[19] Jung, D., Hwang, I., Jo, Y., Jang, C., Han, M., Sunwoo, M., and Chang, J.: In-cylinder pressure-based convolutional neural network for real-time estimation of low-pressure cooled exhaust gas recirculation in turbocharged gasoline direct injec–tion engines. International Journal of Engine Research, 22, 3, 1-12, 2019. doi:10.1177/1468087419879002.

[20] Bermúdez, V., Lujan, M.J., Pla, B., Linares, G.W.: Effects of low-pressure exhaust gas recirculation on regulated and unregulated gaseous emissions during NEDC in a light-duty diesel engine. Energy 36, 5655-5665, 2011.

[21] Joseph, A., Rajeevan, J., Shihabudeen, H., Thampi, G. K. (2016). Approximate analysis of SI engine knocking using wavelet and its control with cooled

exhaust gas recirculation. FME Transactions, 44(1), 22–28. https://doi.org/10.5937/fmet1601022J.

[22] Giechaskiel, B., Zardini, A.A., Clairotte, M.: Ex–haust gas condensation during engine cold start and application of the dry-wet correction factor. App–lied Sciences, 9, 11, 2263, 2019. https://doi.org/10.3390/app9112263.

[23] Siokos, K., Koli, R., Prucka, R., Schwanke, J.: Assessment of Cooled Low Pressure EGR in a Turbocharged Direct Injection Gasoline Engine. SAE International Journal of Engines 8, 4, 2015. https://doi.org/10.4271/2015-01-1253.

[24] Garrido Gonzalez, N., Baar, R., Drueckhammer, J., and Kaeppner, C., The thermodynamics of exhaust gas condensation. SAE International Journal of Engines, 10, 4, 1411-1421, 2017. https://doi.org/10.4271/2017-01-9281.

[25] Serrano, J.R., Piqueras, P., Angiolini, E., Meano, C., Morena, J., On cooler and mixing condensation phenomena in the long-route exhaust gas recir–culation line. SAE Technical Paper, 2015-24-2521, 2015. https://doi.org/10.4271/2015-24-2.

[26] Burson-Thomas, C.B., Harvey, T.J., Fletcher, L., Wellman, R., Pierron, F., Wood, R.J.K. Investi–gating high-speed liquid impingement with full-field measurements. Proceedings of the Royal Society A: Mathematical, Physical and Engineering Sciences, 479, 2277, 20230023, 2023. https://doi.org/10.1098/rspa.2023.0023.

[27] Song H, Song S.: Numerical investigation on a dual loop EGR optimization of a light duty diesel engine based on water condensation analysis. Applied Thermal Engineering, 182, 116064, 2021. https://doi.org/10.1016/j.applthermaleng.2020.116064.

[28] Galindo J, Navarro R, Tarí D, García-Olivas G.: Centrifugal compressor influence on condensation due to long route exhaust gas recirculation mixing. Applied Thermal Engineering, 144, 901-909, 2018. https://doi.org/10.1016/j.applthermaleng.2018.09.005.

[29] #Reihani, A., Hoard, J., Klinkert, S., Kuan, C., Styles, D., McConville, G.: Experimental response surface study of the effects of low-pressure exhaust gas recirculation mixing on turbocharger comp–ressor performance. Applied Energy, 261, 114349, 2020. https://doi.org/10.1016/j.apenergy.2019.114349.

[30] Córdoba, P., Serrano, D., García, R.: Internal com–bustion engines and carbon-neutral fuels: A pers–pective on emission neutrality in the European Union. Energies, 17, 5, 1216, 2024. https://doi.org/10.3390/en17051216.

[31] Abubakar, S., Muhamad Said, M.F., Abas, M.A., Ismail, N.A., Khalid, A.H., Roslan, M.F., Kaisan, M.U.: Hydrogen-fuelled internal combustion engi–nes – Bibliometric analysis on research trends, hot–spots, and challenges. International Journal of Hyd–rogen Energy, 61, 623–638, 2024. https://doi.org/10.1016/j.ijhydene.2024.02.280.

[32] Martins, J., Brito, F.P.: Alternative fuels for internal combustion engines. Energies, 13, 16, 4086. 2020. https://doi.org/10.3390/en13164086.

[33] Moroz, S., Bourgoin, G., Luján, J.M., Pla, B.: Acidic condensation in low pressure EGR systems using diesel and biodiesel fuels. SAE International Journal of Fuels and Lubricants, 2, 2, 305–312, 2010. https://doi.org/10.4271/2009-01-2805.

[34] d'Ambrosio, S., Mancarella, A., Manelli, A.: Utili–zation of hydrotreated vegetable oil (HVO) in a Euro 6 dual-loop EGR diesel engine: Behavior as a drop-in fuel and potentialities along calibration parameter sweeps. Energies, 15, 19, 7202, 2022. https://doi.org/10.3390/en15197202.

[35] Szwaja, S., Piotrowski, A., Szwaja, M., Musial, D.: Thermodynamic analysis of the combustion process in hydrogen-fueled engines with EGR. Energies, 17, 12, 2833, 2024. https://doi.org/10.3390/en17122833.

[36] Johar, T., Hsieh, C.-F.: Design challenges in hyd–rogen-fueled rotary engine - A review. Energies, 16, 2, 607, 2023. https://doi.org/10.3390/en16020 607.

[37] Lide, D.R.: CRC handbook of chemistry and phy–sics, CRC Press, Boca Raton, 2003.

[38] Alduchov, O.A., Eskridge, R.E.: Improved Magnus form approximation of saturation vapor pressure. Journal of Applied Meteorology, 35, 4, 601-609, 1996. https://doi.org/10.1175/1520-0450(1996)035.

[39] Hoppe, F., Thewes, M., Baumgarten, H., Dohmen, J.: Water injection for gasoline engines: Potentials, challenges, and solutions. International Journal of Engine Research, 17, 1, 86–96, 2016. https://doi.org/10.1177/1468087415599867.

[40] Abdelhameed, E., Tashima, H.: EGR and emulsi–fied fuel combination effects on the combustion, performance, and NOx emissions in marine diesel engines. Energies, 16, 1, 336, 2023. https://doi.org/10.3390/en16010336.

[41] Gu, W., Su, W.: Study on the effects of exhaust gas recirculation and fuel injection strategy on transient process performance of diesel engines. Sustaina–bility, 15, 16, 12403, 2023. https://doi.org/10.3390/su151612403.

[42] Coskun, C., Oktay, Z., Ilten, N.: A new approach for simplifying the calculation of flue gas specific heat and specific exergy value depending on fuel composition. Energy, 34, 11, 1898–1902, 2009. https://doi.org/10.1016/j.energy.2009.07.040.

[43] Shepelev, V., Gritsenko, A., Salimonenko, G.: Con-trol of hydrocarbon emissions when changing the technical condition of the exhaust system of modern cars. FME Transactions, 49, 3, 749–755, 2021. https://doi.org/10.5937/fme2103749S.

NOMENCLATURE

BSFC	Brake specific fuel consumption
c_{amb}	Specific heat capacity of ambient air
c_{exh}	Specific heat capacity of exhaust gas
DI	Direct injection
e_{avp}	Actual vapor pressure

HVO	Hydrotreated vegetable oil
HP-EGR	High-pressure Exhaust Gas Recircaulation
LHV	Lower heating value
LP-EGR	Low-pressure Exhaust Gas Recirculation
M	Molecular weight
$\dot{m}_{amb}$	Ambient (Intake) air mass flow
$\dot{m}_{cond}$	Condensate mass flow
$\dot{m}_{fuel}$	Fuel mass flow
$\dot{m}_{ML-EGR}$	LP-EGR mass flow
p_{amb}	Ambient air pressure
$p_{lp\text{-}egr}$	Pressure level in LP-EGR channel
p_{mix}	Pressure level upstream of compressor
R	LP-EGR ratio
T_{amb}	Ambient air temperature
T_{dew}	Dew point temperature
T_{exh}	Exhaust gas temperature
T_{mix}	Temperature of the mixture
VTG	Variable Turbine Geometry
w_{amb}	Specific humidity of ambient air
w_{exh}	Exhaust gas specific humidity
WLTC	Worldwide harmonized Light vehicles Test Cycle
w_{mix}	Specific humidity of the mixture

Greek symbols

λ	Air-to-fuel ratio

Superscripts

C	Compressor
T	Tubrine

КВАНТИТАТИВНА АНАЛИЗА КОНДЕНЗАЦИЈЕ ВОДЕ У ЛП-ЕГР СИСТЕМИМА ЗА МОТОРЕ СА УНУТРАШЊИМ САГОРЕВАЊЕМ

Р. Такач, Ј. Вакула, Ј. Принсиер

Рециркулација издувних гасова ниског притиска (ЛП-ЕГР) је обећавајућа стратегија за смањење емисије NOx у моторима са унутрашњим сагоревањем, али представља изазове због кондензације водене паре која може довести до ерозије импелера компресора. Ова студија представља свеобухватну термодинамичку анализу за квантификацију формирања кондензата и одређивање температуре тачке росе код различитих горива и услова рада мотора. Развијени су нови математички модели за процену специфичне влажности и кондензације користећи само стандардне параметре мотора, што их чини применљивим без додатних сензора.

Резултати показују да и састав горива - посебно однос водоника и угљеника - и брзине ЛП-ЕГР снажно утичу на кондензацију. Студија такође истиче утицај алтернативних горива и услова околине на ризик од кондензације. Развијена методологија подржава процену потенцијала кондензације у реалном времену и нуди кључни допринос за процену ризика од ерозије, дизајн компоненти и оптимизацију стратегије контроле емисија у савременим погонским склоповима.